

Short Communication

A Novel Binder-Free Sulfur/Polypyrrole Cathode for Lithium/Sulfur Batteries

Li Wang¹, Zichuan Yi^{4,5,6}, Xin Wang^{1,3,*}, Yongguang Zhang^{2,*}, Mingliang Jin^{1,3}, Guofu Zhou^{1,5,6}

¹ Institute of Electronic Paper Displays, South China Academy of Advanced Optoelectronics, South China Normal University, Guangzhou, Guangdong Province, China

² Synergy Innovation Institute of GDUT, Heyuan, Guangdong Province, China

³ International Academy of Optoelectronics at Zhaoqing, South China Normal University, National High-Tech Zone, Zhaoqing, Guangdong Province, China

⁴ University of Electronic Science and Technology of China, Zhongshan Institute, Zhongshan 528402, China

⁵ Shenzhen Guohua Optoelectronics Tech. Co. Ltd., Shenzhen 518110, China

⁶ Academy of Shenzhen Guohua Optoelectronics, Shenzhen 518110, China

*E-mail: wangxin@scnu.edu.cn, zyg1984723@hotmail.com

Received: 30 November 2016 / Accepted: 14 April 2017 / Published: 12 May 2017

A novel type cathode for lithium/sulfur batteries is introduced based on polypyrrole nanowires on a Ni foil without any binder. Herein, a facile two-step approach is developed in this paper for the fabrication of novel three-dimensional nanoarchitectures of composite. Polypyrrole nanowires are directly synthesized on the Ni current collector. PPy on Ni foil is utilized as the flexible substrate for the infiltration of S *via* heat-treatment. The S/PPy binary composite electrode delivers a large reversible capacity of 1166 mAh g⁻¹ with appealing cycling stability (57 % capacity retained after 100 cycles). The electrochemical results show that PPy nanowire directly growing on the Ni foil current collector could offer both an electron-conductive path and a stable substrate for the sulfur electrode. Besides, PPy also has strong adhesion to the surface of Ni foil and absorbs polysulfides into its porous structure.

Keywords: Binder-free, Electropolymerized, sulfur/polypyrrole composite, sulfur cathode, lithium/sulfur battery.

1. INTRODUCTION

In recent years, there has been a strong demand to develop electric vehicles (EVs) to save limited resources of fossil fuels and decrease exhaust emissions. Therefore, the development of advanced rechargeable batteries with high-energy density for the EV applications is in great demand

[1,2]. Among the various battery candidates, lithium/sulfur (Li/S) battery has attracted great interest, due to its high theoretical energy density as high as 2600 Wh Kg^{-1} , based on the complete reactions of sulfur with lithium metal to form Li_2S [3,4]. In addition, the cathode material sulfur is an inexpensive, abundant resource, which is environmentally benign [5]. Nevertheless, sulfur cathodes suffer from several significant challenges: low electrical/ionic conductivity and high solubility of polysulfides produced during charge/discharge processes, which overall reduce cell performance. Therefore, a technique for enhancing the conductivity of sulfur cathode as well as immobilizing the polysulfides is highly required [6].

Among the possible strategies, polypyrrole (PPy) has been chosen as polymer additive for sulfur cathode to improve the conductivity, the capacity and cycling durability, owing to its high electrical conduction accompanied by a high stability [7] and high sulfur absorption ability [8]. In our previous studies, branched S/PPy composite and PPy coated sulfur composite has been built respectively, which both showed improved electrochemical performance [9,10]. Furthermore, Liang *et al* prepared a tubular PPy@S@PPy composite cathode, which exhibited better electrochemical stability, cyclability, and rate capability than S@PPy composite counterpart [11].

In a conventionally designed S/PPy composite cathode, polymeric binders are necessary, virtually resulting in an increase of the resistance and electrode polarization. Therefore, a special structure for binder-free sulfur electrodes has to be prepared.

Herein, we develop a novel electropolymerized PPy nanofiber matrix grown on the Ni foil as a flexible substrate for the deposition of sulfur nanoparticle. In this well-designed configuration, sulfur was homogeneously coated on the surface of PPy matrix. The inactive PPy core can conveniently maintain the structural integrity of the composite and facilitate the charge collection and transport. PPy nanofiber also has strong adhesion to the surface of Ni foil and absorb polysulfides into its porous structure. Furthermore, binders and conductive agents are rendered unnecessary in this free-standing S/PPy electrode, thereby simplifying its preparation. And the physical and electrochemical properties of the binder-free S/PPy cathode were investigated for Li/S batteries.

2. EXPERIMENTAL

A three-dimensional PPy nanofiber network was synthesized by electropolymerization of the pyrrole monomer in aqueous solution, and then a binder-free S/PPy electrode was prepared by impregnation of as prepared PPy matrix with elemental melted sulfur.

The three-dimensional PPy nanofibers network was synthesized by electro-polymerization of the pyrrole monomer in aqueous solution as the previous report [12]. Then, PPy nanofibers were rinsed with distilled water and dried at $80 \text{ }^\circ\text{C}$ for 10 h in vacuum. Subsequently, 0.25 M sulfur in CS_2 solution was painted on the substrate of PPy nanofiber network. And, CS_2 was allowed to completely evaporate at $60 \text{ }^\circ\text{C}$ in vacuum. The resulting electrode was heated at $150 \text{ }^\circ\text{C}$ for 3 h in argon gas to obtain a desired binder-free electrode. The sulfur mass loading was 0.4 mg cm^{-2} , which is round 60% of the total mass of the S/PPy nanostructures. X-ray diffraction (XRD) patterns were tested by Bruker D8 advance with $\text{Cu K}\alpha$. The morphologies and microstructures of the samples were characterized using

field-emission scanning electron microscope (FE-SEM, S4800, Hitachi Limited) and transmission electron microscopy (TEM, JEM-2100F, JEOL), respectively.

Coin cell 2025 were assembled with the S/PPy cathode, lithium metal anode and a microporous polypropylene separator in the argon-filled glove box (MBraun). The electrolyte is 1 M $\text{LiN}(\text{CF}_3\text{SO}_2)_2$ in ethylene glycol dimethyl ether and 1,3-dioxolane (1:1 v/v). The coin cells were cycled between 1 and 3 V vs. Li^+/Li at different current densities. Applied currents and specific capacities were calculated on the basis of the weight of S in each cathode.

3. RESULTS AND DISCUSSION

Fig. 1 presents the XRD pattern of PPy grown directly on Ni foil and S/PPy on Ni foil, respectively. Removing strong peaks of the Ni substrate, one can see that PPy has a broad and weak diffraction peak at 25° , indicating an amorphous structure [9]. In comparison, the S/PPy composite showed obvious characteristic diffraction peaks of sulfur (F_{ddd} orthorhombic phase), indicating that no phase transformation of sulfur during the sulfur loading process.

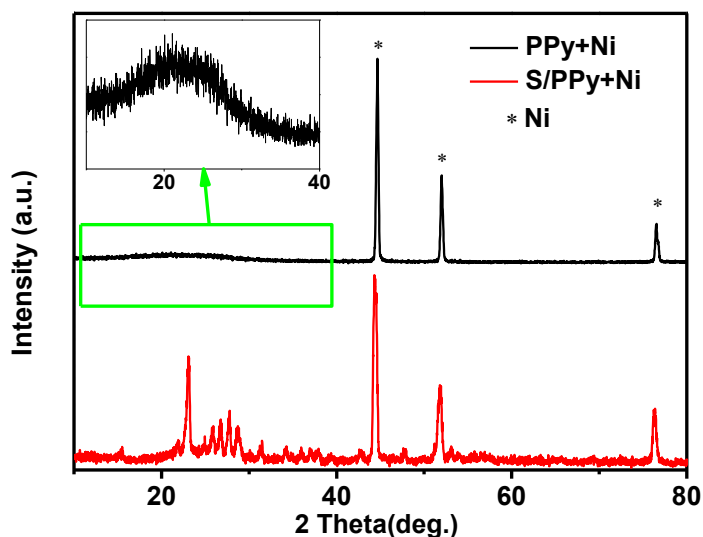


Figure 1. XRD patterns of PPy and S/PPy composite.

The surface morphology of as prepared PPy and S/PPy composite on the Ni foil is depicted in Fig. 2. One can see in Fig. 2a that as prepared PPy demonstrates cross-linked nanofiber structure, and forms a porous interconnected 3D framework. This porous PPy matrix could provide a highly conductive network in conjunction with a large surface area to support good contact with sulfur. As shown in Fig. 2b, sulfur coating process on PPy nanofiber does not bring any structure change except that the average diameter of nanofiber has a significant increase. As expected, no sulfur aggregation is observed. To further investigate the structure of PPy and S/PPy composite, TEM measurement was

conducted. Fig. 2c confirms the nanofiber structure of as-prepared PPy, and at a higher magnification, no obvious lattice fringes can be observed and PPy has the amorphous structure, which is consistent with XRD results. As for S/PPy composite, the core-shell structure of an individual composite nanofiber is identified by Fig. 2d. The elemental mapping of S/PPy carried out by EDS is shown in Fig. 2f, demonstrating the existence and homogeneous distribution of sulfur and PPy in the composite. Furthermore, EDX line scan across the S/PPy shows the variation of sulfur signal as shown in Fig. 2g, which further confirmed the core-shell structure of S/PPy. In the composite, the PPy nanofiber backbones could maintain a good mechanical strength and good contact with sulfur nanoparticles as well as serve directly as electron-conductive transport paths [13].

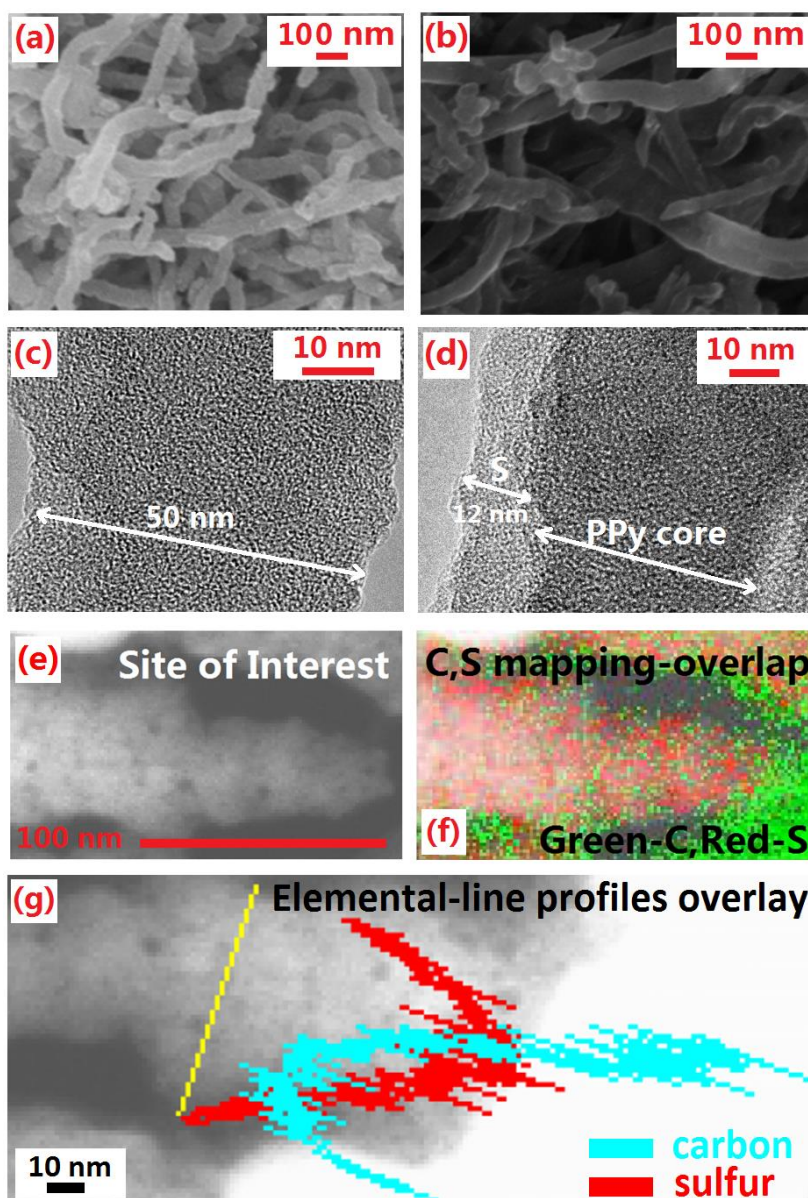
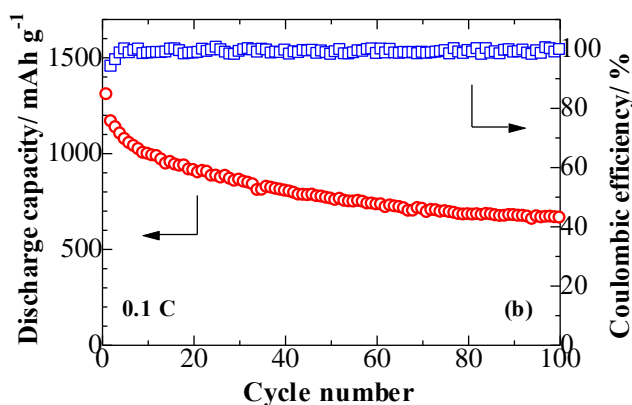
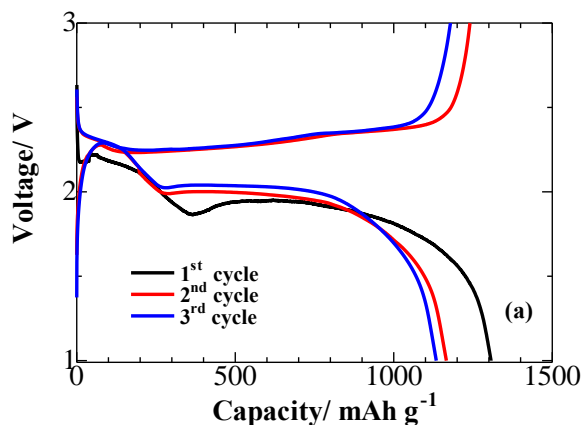


Figure 2. (a,b) SEM images of PPy and S/PPy composite; (c,d) TEM images of PPy and S/PPy composite; (e,f) the elemental mapping for carbon and sulfur; (g) Elemental-line profiles across the S/PPy fiber, showing the distribution of carbon and sulfur.

Electrochemical performances in cells with Li foil anodes and S/PPy composite cathode show very promising performance characteristics. Fig. 3a shows the initial three discharge/charge curves of S/PPy cathode at a rate of 0.1 C. All three discharge curves show similar behaviors, and two voltage plateaus at 2.4 V and 2.0 V are observed, which could be attributed to a two-step reaction of sulfur with lithium. The first plateau at 2.4 V can be assigned to the reduction of elemental S to higher-order lithium polysulfides (Li_2S_n , $4 \leq n \leq 8$). The following electrochemical transition of these polysulfides into lithium sulfides ($\text{Li}_2\text{S}_2/\text{Li}_2\text{S}$) corresponds to the plateau at 2.0 V [14]. The charge/discharge curves of the 2nd and 3rd cycles almost coincide with each other, confirming high reversible and electrochemical stability of the cathode. The S/PPy cathode exhibits outstanding cycle performance as shown in Fig. 3b. The S/PPy composite delivers a high discharge capacity of 1166 mAh g^{-1} in the 2nd cycle at 0.1 C, and the cell could maintain a reversible capacity of 663 mAh g^{-1} after 100 cycles. Furthermore, the S/PPy cathode maintain a high coulombic efficiency about 100% over 100 cycles. This indicates that this unique structure of S/PPy electrode is quite effective in suppressing the diffusion of polysulfide species and maintaining high utilization of sulfur in the redox reactions [12].

The S/PPy composite were tested at a rate from 0.1 C to 1.5C and back to 0.1 C, to evaluate the kinetics of the cathodes as shown in Fig. 3c. Stable capacities of around 1024, 822, 606 and 497 mAh g^{-1} were obtained at 0.1, 0.5, 1 and 1.5 C, respectively. What's more, when the current rate is changed back to 0.5 C, a discharge capacity of 851 mAh g^{-1} is recovered, indicating structural stability and fast dynamic reaction process of the cathode materials.



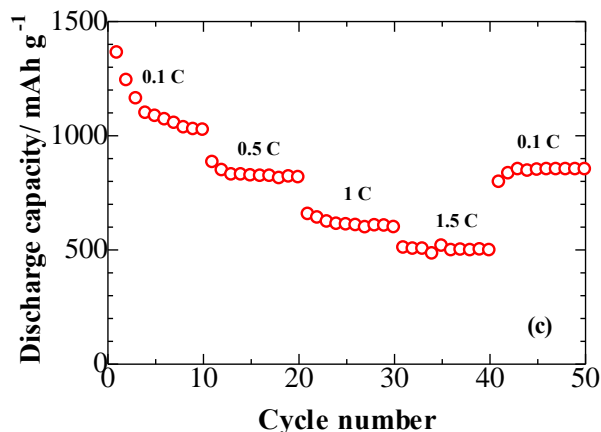


Figure 3. (a) Discharge/charge profiles of the S/PPy composite cathode at 0.1 C; (b) Cyclability of the S/PPy composite cathode at 0.1 C; (c) Rate capability of the S/PPy composite cathode.

According to above results, we tentatively attribute the good rate capability of S/PPy composite electrodes to its unique 3D networked structure, which could shorten the transport length for Li ions, thereby facilitating Li storage kinetics and rate capability [15].

The S/PPy electrodes prepared in this work, exhibits a remarkably enhanced electrochemical performance over most of the earlier S/PPy electrodes reported in literature, as shown in Table 1.

Table 1. Comparison of various S/PPy electrodes for Li-ion batteries.

Material	Reversible capacity	Cycle number	Current density	Ref.
S/PPy/GNS composite	641.5 mAh g ⁻¹	40th	0.1C	[8]
S/PPy nanocomposite	~500 mAh g ⁻¹	40th	100 mA g ⁻¹	[9]
PPy@S@PPy composite	554 mAh g ⁻¹	50th	50 mA g ⁻¹	[11]
Sulfur-polypyrrole composite	~500 mAh g ⁻¹	30th	100 mA g ⁻¹	[16]
Polypyrrole-coated sulfur nanocomposite	613 mAh g ⁻¹	50th	0.1C	[17]
S/T-PPy composite	500 mAh g ⁻¹	60th	0.1 mA cm ⁻²	[18]
S/PPy/MWNT composite	751 mAh g ⁻¹	100th	0.2 C	[19]
S/PPy/MWNT composite	960.7 mAh g ⁻¹	40th	0.1C	[20]
S/PPy composite	1166 mAh g ⁻¹	2th	0.1 C	our work
	663 mAh g ⁻¹	100th	0.1 C	

4. CONCLUSIONS

In summary, a binder-free S/PPy composite electrode has successfully been prepared *via* a facile two-step approach. In this composite, the PPy nanofiber backbones could maintain a good mechanical strength and provide rich accessible electroactive site and short ion transport pathways.

Meanwhile, the highly porous PPy network can effectively confine polysulfides and alleviate the volume expansions of sulfur upon cycles. As results, the S/PPy composite electrode exhibited a stable cycle performance as well as remarkable rate capability. We believe that this binder-free S/PPy electrodes are expected to open up new opportunities for Li/S batteries to eventually in the practical application as new-generation energy storage system.

ACKNOWLEDGEMENTS

The authors acknowledge the financial support from the National Key Research and Development Program of China (NO.2016YFB0401502), the National Natural Science Foundation of China (Grant No. 51602111, 51561135014), Guangdong Province Grant NO. 2014A030308013, 2014B090915005, 2015A030310196, 2015B050501010, 14KJ13, the Pearl River S&T Nova Program of Guangzhou (201506040045), Guangdong Innovative Research Team Program (No. 2013C102), PCSIRT Project No. IRT13064, and supported by the 111 Project.

References

1. P.G. Bruce, S.A. Freunberger, L.J. Hardwick and J.M. Tarascon, *Nature Mater*, 11 (2011) 19.
2. Y. Zhao, F.X. Yin, Y.G. Zhang, C.W. Zhang, A. Mentbayeva and N. Umirov, *Nanoscale Res Lett*, 10 (2015) 1.
3. Y. Yang, G. Zheng, S. Misra, J. Nelson, M.F. Toney and Y. Cui, *J Amer Chem Soc*, 134 (2012) 15387.
4. R.Q. Wang, Y.L. Zhao and B.F. Xie, *Electrochim Acta*, 143 (2014) 49.
5. D. Bresser, S. Passerini and B. Scrosati, *Chem Commun*, 49 (2013) 10545.
6. A. Konarov, D. Gosselink, T. N. L. Doan, Y.G. Zhang, Y. Zhao and P. Chen, *J Power Sources*, 259 (2014) 183.
7. Y.P. Xie, H.B. Zhao, H.W. Cheng, C.J. Hu, W.Y. Fang, J.H. Fang, J.Q. Xu and Z.W. Chen, *Appl Energy*, 175 (2016) 522.
8. Y.G. Zhang, Y. Zhao, A. Konarov, D. Gosselink, H.G. Soboleski and P. Chen, *J. Power Sources*, 241 (2013) 517.
9. Y.G. Zhang, Z. Bakenov, Y. Zhao, A. Konarov, T.N.L. Doan, M. Malik, T. Paron and P. Chen, *J Power Sources*, 208 (2012) 1.
10. Y.G. Zhang, Y. Zhao, A. Konarov, D. Gosselink, Z. Li, M. Ghaznavi and P. Chen, *J Nanopart. Res*, 15 (2013) 1.
11. X. Liang, M. Zhang, M.R. Kaiser, X. Gao, K. Konstantinov, R. Tandiono, Z.X. Wang, H.K. Liu, S.X. Dou and J.Z. Wang, *Nano Energy*, 11 (2015) 587.
12. Z. Du, S. Zhang, Y. Liu, J. Zhao, R. Lin and T. Jiang, *J Mater Chem*, 22 (2012) 11636.
13. A. Mentbayeva, A. Belgibayeva, N. Umirov, Y. Zhang, I. Taniguchi and I. Kurmanbayeva, *Electrochim Acta*, 217 (2016) 242.
14. Y. Zhao, Z. Bakenova, Y. Zhang, H. Peng, H. Xie and Z. Bakenov, *Ionics*, 21 (2015) 1925.
15. H.P. Li, Y.Q. Wei, Y.G. Zhang, C.W. Zhang, G.K. Wang and Y. Zhao, *Ceram Int*, 42 (2016) 12371.
16. J.E. Hyun, P.C. Lee, I. Tatsumi, *Electrochim. Acta*, 176 (2015) 887.
17. G. Yuan, H. Wang, *J. Energ. Chem.*, 23 (2014) 657.
18. X. Liang, Z. Wen, Y. Liu, X. Wang, H. Zhang, M. Wu, L. Huang, *Solid State Ionics*, 192 (2011) 347.
19. Y. Zhang, Y. Zhao, Z. Bakenov, M. Tuiyebayeva, A. Konarov, P. Chen, *Electrochim. Acta*, 143 (2014) 49.
20. Y. Zhang, Y. Zhao, T.N.L. Doan, A. Konarov, D. Gosselink, H.G. Soboleski, P. Chen, *Solid State*

Ionics, 238 (2013) 30.

© 2017 The Authors. Published by ESG (www.electrochemsci.org). This article is an open access article distributed under the terms and conditions of the Creative Commons Attribution license (<http://creativecommons.org/licenses/by/4.0/>).